

# UTILIZATION OF HEMIHYDRATE PHOSPHOGYPSUM FOR THE PREPARATION OF ENERGY EFFICIENCY WALL MATERIALS

ZHANG YICHAO, WANG YING, ZHOU JINGHAI, KANG TIANBEI, WANG QINGHE \*

School of Civil Engineering, Shenyang Jianzhu University, Shenyang 110000, China

*Phosphogypsum is a byproduct of the manufacture of phosphoric acid by dehydrating process. The discarded phosphogypsum not only occupies considerable land resource, but also leads to serious environmental contamination. In order to improve the utilization rate of phosphogypsum, hemihydrate phosphogypsum was used as raw materials for manufacturing energy efficiency wall materials in this paper. Comparing with the conventional structure, the optimized structure was designed based on energy efficiency wall materials. The heat transfer of optimized structure was simulated to evaluate the energy efficiency of wall. The results show that the prepared material has suitable setting time, compressive strength and low thermal conductivity. Two-dimensional heat transfer coefficient of thermal bridge is decreased by 18.5%, and the average heat transfer coefficient of wall structure is decreased by 13.9%. The optimized structure can effectively improve the thermal insulation properties of walls.*

**Keywords:** Hemihydrate phosphogypsum, vitrified microsphere, energy efficiency wall materials, heat transfer characteristic

## 1. Introduction

Phosphogypsum (PG) is a byproduct of the manufacture of phosphoric acid by dehydrating process [1,2]. About five tons of PG is generated per ton of phosphoric acid production. Global PG emissions have exceeded 150 million tons every year. In China, the annual emissions in PG are more than 55 million tons [3-6]. The utilization proportion of PG is less than 10% in China. The discarded PG not only occupies considerable land resource, but also leads to serious environmental contamination.

Strong efforts have been made in the systematic utilization of PG. Such as using PG as set retarders [7,8], gypsum binders [9-11], gypsum plasters [12-16] and so on. However, in most of the existing studies, the consumption of PG is not large. Moreover, the thermal insulation properties of the products are not emphasized, which are the concerns of residential buildings.

In this work, hemihydrate PG was used as raw materials for manufacturing energy efficiency wall materials (EEWM). Two-dimensional heat transfer theory was analyzed based on additional heat loss of thermal bridge and two-dimensional heat transfer characteristic of thermal bridge. Comparing with the conventional structure, the optimized structure was designed based on the prepared material. The heat transfer of optimized structure was simulated to evaluate the energy efficiency of wall.

## 2. Experimental

### 2.1 Raw materials

$\beta$ -hemihydrate phosphogypsum, fly ash, vitrified microsphere, protein based retarder (SSP),

polycarboxylate based plasticizer (F10) were used in this work.  $\beta$ -hemihydrate phosphogypsum was taken from phosphate fertilizer plant in Hubei province, China. The initial and final setting time was 4min and 8min respectively, and the 28d compressive strength was 3.72MPa, and the thermal conductivity was 0.25W/(m•K). Irradiation index of  $\beta$ -hemihydrate phosphogypsum was tested according to the Chinese standard (GB 6566-2010) [17]. The test showed that natural radionuclide radium, thorium, potassium were 38Bq/kg, 42Bq/kg, 330Bq/kg respectively. The internal and external irradiation indexes were 0.19 and 0.34 respectively, which meet the requirements of radionuclide limit of wall materials. Fly ash, vitrified microsphere were taken from power plant in Hubei province, China, and the thermal conductivity was 0.23W/(m•K) and 0.04W/(m•K) respectively.

### 2.2 Mix proportions

Cementitious materials were composed of  $\beta$ -hemihydrate phosphogypsum and fly ash. Vitrified microsphere, protein based retarder and polycarboxylate based plasticizer were added into cementitious materials as additives. The content of  $\beta$ -hemihydrate phosphogypsum, fly ash, vitrified microsphere, protein based retarder and polycarboxylate based plasticizer were designed as 70%/80%, 20%/30%, 10%/20%, 0.1%/0.2% and 0.2%/0.3% respectively. Sixteen mix proportions were designed, as shown in Table 1.

### 2.3 Test methods

#### 2.3.1 Setting time

The setting time was tested according to the Chinese standard (GB/T 17669.4-1999) [18]. The

\* Autor corespondent/Corresponding author,  
E-mail: wangqinghe@sjzu.edu.cn

Table 1

Mix proportions of EEWM						
No.	$\beta$ -hemihydrate phosphogypsum (%)	Fly ash (%)	Vitrified microsphere (%)	Protein based retarder (%)	Polycarboxylate based plasticizer (%)	
1	70	30	10	0.1	0.2	
2	70	30	20	0.1	0.2	
3	70	30	10	0.1	0.3	
4	70	30	20	0.1	0.3	
5	70	30	10	0.2	0.2	
6	70	30	20	0.2	0.2	
7	70	30	10	0.2	0.3	
8	70	30	20	0.2	0.3	
9	80	20	10	0.1	0.2	
10	80	20	20	0.1	0.2	
11	80	20	10	0.1	0.3	
12	80	20	20	0.1	0.3	
13	80	20	10	0.2	0.2	
14	80	20	20	0.2	0.2	
15	80	20	10	0.2	0.3	
16	80	20	20	0.2	0.3	

time interval was 2min. The size of the specimen was 65×75×40mm.

### 2.3.2 Diffusance

The diffusance was tested according to the Chinese standard (GB/T 28627-2012) [19] in order to evaluate the fluidity of materials.

### 2.3.3 Compressive strength

The compressive strength was tested according to the Chinese standard (GB/T 17669.3-1999) [20]. The size of the specimen was 40×40×160mm.

### 2.3.4 Thermal conductivity

The thermal conductivity was tested according to the Chinese standard (GB/T 10294-2008) [21]. In the test, an intelligent double-plate detector (IMDRY3001) was used to determine the heat flow through the specimen, the average temperature of hot surface, and the average temperature of cold surface. The size of the specimen was 300×300×30mm.

## 3. Results and discussion

### 3.1 Effect of components on setting time

The setting time of EEWM with different mix proportions were tested, as shown in Table 2. As is shown in Table 2, when the content of fly ash, vitrified microsphere and plasticizer are the same, the setting time of EEWM is increasing with the increase of the retarder content. When the content of fly ash, retarder and plasticizer are the same, the setting time of EEWM is decreasing with the increase of the vitrified microsphere content. The results show that the setting time of EEWM is mainly affected by retarder and vitrified microsphere. And it shows that the influence of retarders on the setting time of EEWM is greater than that of vitrified microsphere. The main

mechanism of retarder is to slow down the dissolution rate of hemihydrate phosphogypsum, resulting in increasing the setting time. When the content of retarder is 0.1%, the initial setting time of EEWM is 44-58min, and the final setting time is 54-66min. When the content of retarder is 0.2%, the initial setting time of EEWM is 72-84min, and the final setting time is 78-90min.

### 3.2 Effect of components on diffusance

The diffusance of EEWM with different mix proportions were tested, as shown in Table 2. As is shown in Table 2, when the content of plasticizer is 0.2%, the diffusance of EEWM is 198-202mm. When the content of plasticizer is 0.3%, the diffusance of EEWM is 218-223mm. The diffusance of EEWM is mainly affected by plasticizer.

### 3.3 Effect of components on compressive strength

The 28d compressive strength of EEWM with different mix proportions were tested, as shown in Table 2. As is shown in Table 2, when the content of vitrified microsphere is the same, the compressive strength of specimen is smaller with the retarder content 0.2%. When the content of retarder is the same, the compressive strength of specimen is greater with vitrified microsphere content 20%. It shows that the compressive strength of EEWM is mainly affected by retarder and vitrified microsphere. When the content of fly ash and plasticizer are the same, the compressive strength of EEWM is decreasing with the content of retarder and vitrified microsphere increasing simultaneously. It shows that the effect of retarder on the compressive strength of EEWM is greater than that of vitrified microsphere. The compressive strength of EEWM decreases with the increase of retarder, which is mainly due to the change of the shape of gypsum crystal. During the hydration of gypsum, the shape of crystals is changed from

Table 2

Specimen No.	Setting time(min)		Diffusance (mm)	28d compressive strength(MPa)	Thermal conductivity (W/(m•K))
	Initial(min)	Final(min)			
1	58	66	200	2.76	0.152
2	48	56	198	2.98	0.132
3	56	64	221	2.34	0.155
4	46	54	220	3.05	0.131
5	84	90	201	1.30	0.154
6	74	82	199	1.60	0.132
7	80	88	223	1.36	0.155
8	72	78	220	2.00	0.133
9	56	66	198	2.55	0.156
10	46	58	200	2.75	0.135
11	56	62	221	2.65	0.153
12	44	54	222	2.87	0.133
13	84	88	202	1.60	0.152
14	74	80	200	2.16	0.134
15	80	88	218	1.78	0.156
16	72	80	221	1.88	0.132

needle to columnar due to the adsorption of retarder, and the overlaps between the crystals are reduced, so the compressive strength of EEWM is reduced.

**3.4 Effect of components on thermal conductivity**

The thermal conductivity of EEWM with different mix proportions were tested, as shown in Table 2. As is shown in Table 2, the thermal conductivity of EEWM is mainly affected by vitrified microsphere. The vitrified microspheres are irregular spherical particles with cavity structure. By incorporating vitrified microsphere into cementitious materials, the path of heat conduction can be increased, and then the thermal conductivity of the materials can be reduced. When the content of vitrified microsphere is 10%, the thermal conductivity of EEWM is 0.152-0.156W/(m•K). When the content of vitrified microsphere is 20%, the thermal conductivity of EEWM is 0.131-0.135W/(m•K).

**3.5 Analysis of heat transfer characteristic of structure based on EEWM**

**3.5.1 Two-dimensional heat transfer theory**

**3.5.1.1 Additional heat loss of thermal bridge**

The additional heat loss of thermal bridge is evaluated mainly through the additional heat loss degree of thermal bridge and the additional heat loss degree of influence area of thermal bridge. The additional heat loss degree of thermal bridge is defined as the ratio of the additional heat flux of thermal bridge to the total heat flux of wall structure. The additional heat loss degree of influence area of thermal bridge is defined as the ratio of additional heat flux of influence area of thermal bridge to the additional heat flux of thermal bridge, shown in formula (1) and (2). The total heat flux of wall structure, additional heat flux of thermal bridge and additional heat flux of influence area of thermal bridge is calculated by the formula (3), (4), (5).

$$\alpha = \frac{\Delta Q_B}{Q_{sum}} \times 100\% \tag{1}$$

$$\beta = \frac{\Delta Q_{Bex}}{\Delta Q_B} \times 100\% \tag{2}$$

$$Q_{sum} = \int_{F_m} q dx \tag{3}$$

$$\Delta Q_B = Q_{sum} - q_p \cdot F_m \tag{4}$$

$$\Delta Q_{Bex} = \int_{F_{pw}} (q - q_p) dx \tag{5}$$

In the formula,  $\alpha$ —additional heat loss degree of thermal bridge (%),  $\beta$ —additional heat loss degree of influence area of thermal bridge (%),  $Q_{sum}$ —total heat flux of wall structure (W),  $\Delta Q_B$ —additional heat flux of thermal bridge (W),  $\Delta Q_{Bex}$ —additional heat flux of influence area of thermal bridge (W),  $q$ —heat flow density at any point of wall structure (W/m<sup>2</sup>),  $q_p$ —heat flux density of wall structure (W/m<sup>2</sup>),  $F_m$ —total area of wall structure (m<sup>2</sup>),  $F_{pw}$ —area of influence area of thermal bridge (m<sup>2</sup>).

When calculating the heat loss parameters of thermal bridge of wall structure, the total heat flux of wall structure is calculated firstly, then the additional heat flux of thermal bridge and the additional heat flux of influence area of thermal bridge are calculated. Finally, additional heat loss degree of thermal bridge and additional heat loss degree of influence area of thermal bridge are determined by the heat flux of each part, and the thermal insulation performance of thermal bridge can be evaluated.

**3.5.1.2 Two-dimensional heat transfer of thermal bridge**

The calculation method of two-dimensional heat transfer coefficient of thermal bridge is

proposed. The two-dimensional heat transfer coefficient of thermal bridge is an indicator to evaluate the heat transfer of thermal bridge considering the additional heat flux of thermal bridge and the additional heat flux of influence area of thermal bridge. According to the heat transfer theory, two-dimensional heat transfer coefficient of thermal bridge is expressed as:

$$K_w' = \frac{Q_{sum} - Q_p}{F_w \Delta T} \quad (6)$$

( $Q_{sum} - Q_p$ ) is the total heat flux of thermal bridge in the condition of two-dimensional heat transfer. The relationship between the total heat flux of thermal bridge and the additional heat flux of thermal bridge is established:

$$Q_{sum} - Q_p = q_p F_w + \Delta Q_B + \Delta Q_{Bex} \quad (7)$$

Two-dimensional heat transfer coefficient of thermal bridge is expressed as:

$$K_w' = \frac{q_p F_w + \Delta Q_B + \Delta Q_{Bex}}{F_w \Delta T} \quad (8)$$

Through two-dimensional heat transfer coefficient of thermal bridge, the two-dimensional heat transfer characteristic of thermal bridge can be effectively analyzed, providing a theoretical basis for the study of thermal bridge.

**3.5.2 FEM model based on EEWM**

In FEM model, the length of shear wall and infilling wall was 1000mm and 1000mm respectively, and the thickness was 280mm. The length of insulation board extended to the filling wall was 280mm according to the analysis of

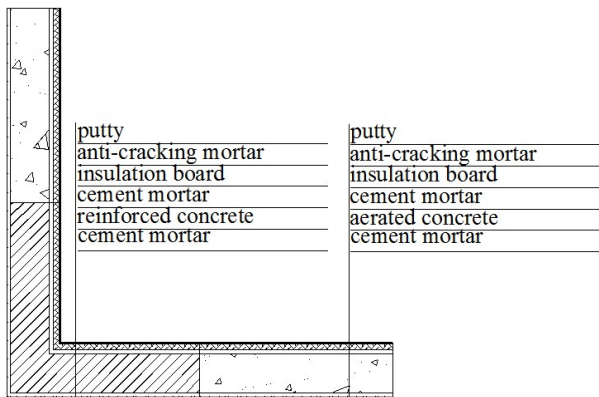


Fig. 1 - FEM model of conventional structure.

influence area of thermal bridge. FEM models of conventional structure and optimized structure were shown in Fig. 1 and Fig. 2.

The convection heat transfer coefficient of the model was 8.7W/(m<sup>2</sup>·K) and the temperature was 18.0°C. The convection heat transfer coefficient on the other side of the model was 23.0W/(m<sup>2</sup>·K) and the temperature was -3.0°C [22]. The thermal conductivity of EEWM in the condition of natural environment was adopted as 0.16W/(m·K). The thermal conductivity of material was shown in Table 3.

**3.5.3 Analysis of additional heat loss of thermal bridge**

Based on the theory of two-dimensional heat transfer coefficient of thermal bridge, the finite element model was calculated using ANSYS. Temperature cloud of conventional structure and optimized structure were shown in Fig. 3 and Fig. 4. Through the extraction of data, the additional heat loss parameters of structures were shown in Table 4. As is shown in Table 4, the additional heat loss of thermal bridge is decreased from 10.11W to 7.22W, and the additional heat loss of influence area of thermal bridge is decreased from 0.76W to 0.12W. It shows that the optimized structure based on EEWM has better thermal insulation capacity of thermal bridge.

**3.5.4 Analysis of heat transfer characteristic of structure**

Through the extraction of data, the heat transfer characteristic indicators of structures were shown in Table 5. The additional heat loss degree of thermal bridge is decreased from 27.0% to 23.0%, and the additional heat loss degree of influence area of thermal bridge is decreased from

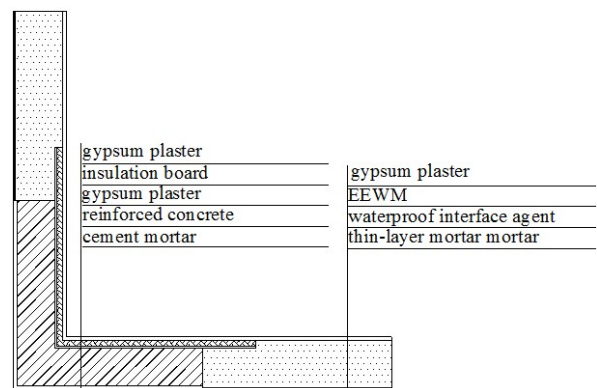


Fig. 2 - FEM model of optimized structure.

**Table 3**

Thermal conductivity of material					
Materials	Reinforced concrete	Insulation board	Cement mortar	Anti-cracking mortar	EEWM
Thermal conductivity (W/(m·K))	1.74	0.038	0.93	0.87	0.16

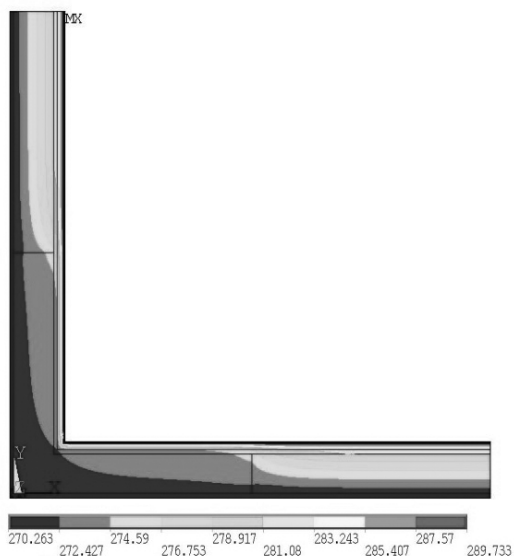


Fig. 3 - Temperature cloud of conventional structure.

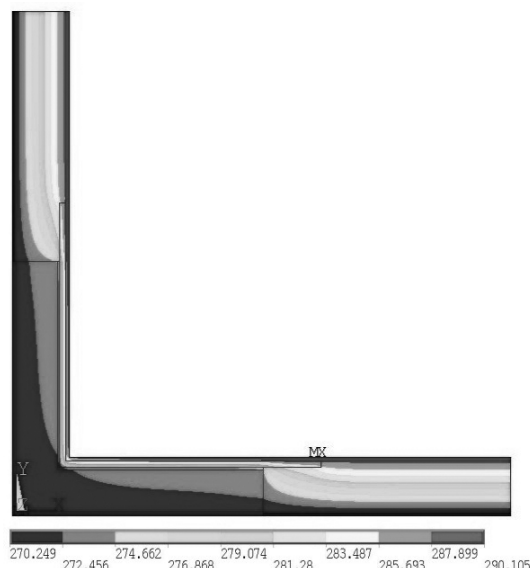


Fig. 4 - Temperature cloud of optimized structure.

Table 4

Additional heat loss parameters of structures					
Parameters	$q_p(W/m^2)$	$q_w(W/m^2)$	$Q_{sum}(W)$	$\Delta Q_B(W)$	$\Delta Q_{Bex}(W)$
conventional	12.32	22.21	36.48	10.11	0.76
optimized	11.41	18.32	31.26	7.22	0.12

Table 5

Heat transfer characteristic indicators of structures				
Indicators	$\alpha(\%)$	$\beta(\%)$	$K_w'(W/(m^2 \cdot K))$	$K_m(W/(m^2 \cdot K))$
conventional	27.0	7.5	1.08	0.79
optimized	23.0	1.7	0.88	0.68

7.5% to 1.7%. Moreover, two-dimensional heat transfer coefficient of thermal bridge is decreased by 18.5%, and the average heat transfer coefficient of wall structure is decreased by 13.9%. The optimized structure can effectively improve the thermal insulation properties of walls.

#### 4. Conclusions

Utilization of hemihydrate phosphogypsum as raw materials in energy efficiency wall materials is feasible and valuable for environment protecting. Based on the experimental results, the following conclusions should be drawn:

The setting time of EEWM is mainly affected by retarder and vitrified microsphere. The effect of retarder on the compressive strength of EEWM is greater than that of vitrified microsphere. When the content of vitrified microsphere is 10%, the thermal conductivity of EEWM is 0.152-0.156W/(m•K), which realizes the preparation of energy efficiency wall materials.

Two-dimensional heat transfer theory is analyzed based on additional heat loss of thermal bridge and two-dimensional heat transfer of thermal bridge. Two-dimensional heat transfer coefficient of thermal bridge is proposed. Comparing with the conventional structure, the

optimized structure is designed based on EEWM. Two-dimensional heat transfer coefficient of thermal bridge is decreased by 18.5%, and the average heat transfer coefficient of wall structure is decreased by 13.9%. The optimized structure based on EEWM can effectively improve the thermal insulation properties of walls. In the future, the energy-saving effect of the whole building using EEWM needs further study.

#### FUNDING

Financial supports from the National Natural Science Foundation of China (51678374, 51808351), the National Key R&D Program of China (2016YFC0700905-04) and Liaoning Basic Scientific Plan (LJZ2017021) were gratefully acknowledged.

#### REFERENCES

- [1]M.Contreras, S.R.Teixeira, G.T.A.Santos, M.J.Gázquez, M.Romero, J.P.Bolívar. Influence of the addition of phosphogypsum on some properties of ceramic tiles. Construction and Building Materials 2018, **175**, 588-600.
- [2]M. P. Campos, L. J. P. Costa, M. B. Nisti, B. P. Mazzilli. Phosphogypsum recycling in the building materials industry: assessment of the radon exhalation rate. Journal of Environmental Radioactivity 2017, **172**, 232-236.
- [3]Francisco Macías, Rafael Pérez-López, Carlos R. Cánovas, Sergio Carrero, Pablo Cruz-Hernandez. Environmental assessment and management of phosphogypsum according to European and United States of America regulations.

Procedia Earth and Planetary Science 2017, **17**, 666-669.

[4]Alaa M. Rashad. Phosphogypsum as a construction material. Journal of Cleaner Production 2017, **166**, 732-743.

[5]Rakesh Kumar Dutta, Vishwas Nandkishor Khatri, Varun Panwar. Strength characteristics of fly ash stabilized with lime and modified with phosphogypsum. Journal of Building Engineering 2017, **14**, 32-40.

[6]D. Nizevičienė, D. Vaičiukynienė, V. Vaitkevičius, Ž. Rudžionis. Effects of waste fluid catalytic cracking on the properties of semi-hydrate phosphogypsum. Journal of Cleaner Production 137, **20**, 150-156.

[7]İ Akın Altun, Yesim Sert. Utilization of weathered phosphogypsum as set retarder in Portland cement. Cement and Concrete Research 2004, **34**(4), 677-680.

[8]J. H. Potgieter, S. S. Potgieter, R. I. McCrindle, C. A. Strydom. An investigation into the effect of various chemical and physical treatments of a South African phosphogypsum to render it suitable as a set retarder for cement. Cement and Concrete Research 2003, **33**(8), 1223-1227.

[9]Guanzhao Jiang, Aixiang Wu, Yiming Wang, Wentao Lan. Low cost and high efficiency utilization of hemihydrate phosphogypsum: Used as binder to prepare filling material. Construction and Building Materials 2018, **167**, 263-270.

[10]T. Kuryatnyk, C. Angulski da Luz, J. Ambroise, J. Pera. Valorization of phosphogypsum as hydraulic binder. Journal of Hazardous Materials 2008, **160**(2-3), 681-687.

[11]Mridul Garg, Neeraj Jain, Manjit Singh. Development of alpha plaster from phosphogypsum for cementitious binders. Construction and Building Materials 2009, **23**(10), 3138-3143.

[12]Manjit Singh. Role of phosphogypsum impurities on strength and microstructure of selenite plaster. Construction and Building Materials 2005, **19**(6), 480-486.

[13]Mridul Garg, Neeraj Jain, Manjit Singh. Development of alpha plaster from phosphogypsum for cementitious binders. Construction and Building Materials 2009, **23**(10), 3138-3143.

[14]Manjit Singh. Treating waste phosphogypsum for cement and plaster manufacture. Cement and Concrete Research 2002, **32**(7), 1033-1038.

[15]Manjit Singh, Mridul Garg. Study on anhydrite plaster from waste phosphogypsum for use in polymerised flooring composition. Construction and Building Materials 2005, **19**(1), 25-29.

[16]Manjit Singh. Effect of phosphatic and fluoride impurities of phosphogypsum on the properties of selenite plaster. Cement and Concrete Research 2003, **33**(9), 1363-1369.

[17]GB 6566-2010. Limits of radionuclides in building materials. (Chinese standard).

[18]GB/T 17669.4-1999. Gypsum plasters- Determination of physical properties of pure past. (Chinese standard).

[19]GB/T 28627-2012. Gypsum plaster. (Chinese standard).

[20]GB/T 17669.3-1999. Gypsum plasters- Determination of mechanical properties. (Chinese standard).

[21]GB/T 10294-2008. Thermal insulation- Determination of steady-state thermal resistance and related properties- Guarded hot plate apparatus. (Chinese standard).

[22]GB 50176-1993. Code for thermal design of civil buildings. (Chinese standard).

\*\*\*\*\*

## MANIFESTĂRI ȘTIINȚIFICE / SCIENTIFIC EVENTS



### 39<sup>th</sup> Cement and Concrete Science Conference

09.09 – 10.09.2019

University of Bath, UK

Topics including but not limited to:

- Hydration and microstructure of cementitious materials
- Alternative cementitious materials and their applications
- Durability of concrete
- Nuclear waste immobilisation
- Atomistic modelling of cements and concrete
- Cement manufacture and low carbon technologies
- Structural and thermal performance of concrete
- Measurement techniques and simulation methods
- Utilisation of waste materials in cementitious materials
- Cementitious materials for 3D printing Applications

\*\*\*\*\*